DOPING EFFECT OF ZrO_2 ON MICROSTRUCTURAL AND ELECTRICAL PROPERTIES OF ZnO–Pr_6O_{11}-BASED CERAMIC VARISTORS

#XIULI FU*, HAI FENG*, **, RUICHAO GAO*, **, ZHIJIAN PENG**

*State Key Laboratory of Information Photonics and Optical Communications, and School of Science, Beijing University of Posts and Telecommunications, Beijing 100876, P. R. China
**School of Engineering and Technology, China University of Geosciences, Beijing 100083, P. R. China

#E-mail: xiulifu@bupt.edu.cn

Submitted May 15, 2015; accepted July 13, 2015

Keywords: ZnO varistor, Pr_6O_{11}, ZrO_2 doping, Electrical properties

ZnO–Pr_6O_{11}–CoO-Cr_2O_3-based ceramic varistors doped with 0-2.0 mol. % ZrO_2 were fabricated via conventional ceramic processing by sintering at 1300°C for 2 h. X-ray diffraction results indicate that the doped ZrO_2 reacted with praseodymium oxides during sintering, resulting in $Pr_2Zr_2O_7$ phase. Scanning electron microscopy analysis revealed that after the addition of ZrO_2, the growth of ZnO grains was inhibited due to the formation of $Pr_2Zr_2O_7$. When the amount was less than 0.5 mol. %, ZrO_2 doping was beneficial for increasing the varistor nonlinear exponent. The varistor voltage increased with increasing ZrO_2 contents in the ceramics, but the leakage current also increased with it. In this work, the sample doped with 0.5 mol. % ZrO_2 presented the highest nonlinear exponent (17), and its varistor voltage was 623 $V \cdot mm^{-1}$. The sample with 2.0 mol. % ZrO_2 presented the highest varistor voltage (1490 $V \cdot mm^{-1}$), and its nonlinear exponent was 10. The obtained varistor would be very promising in super-high-voltage power transmission systems.

INTRODUCTION

ZnO varistors are electronic ceramic devices produced by sintering ZnO powder with small amounts of various metal oxides, which were announced by Matsuoka in 1969 and are still being actively investigated today [1, 2]. They can be used in AC or DC fields over a wide range of voltages, from a few volts to tens of kilovolts, and a wide range of currents, from microamperes to kiloamperes. Their versatility has made ZnO varistors widely applied both in power industry as well as in semiconductor industry [1, 2].

Today the majority of ZnO ceramic varistors are doped with Bi_2O_3 as varistor-forming oxide (VFO), referred as to ZnO–Bi_2O_3-based varistor, which is the commercially commonest composition for ZnO varistor [1]. However, Bi_2O_3 has too much high volatility and reactivity during liquid phase sintering; the former would change the composition ratio of additives and the latter destroy the multilayer structure of chip varistors [3, 4].

To avoid such problems of ZnO–Bi_2O_3-based ceramic varistors, ZnO varistor ceramics containing Pr_6O_{11} as VFO have been actively and extensively studied [3-12]. It was first reported by Mukae et al. that ZnO ceramics containing Pr_6O_{11} and Co_3O_4 could exhibit nonohmic characteristics, referred as to ZnO–Pr_6O_{11}-based ceramic varistors. Such varistors have a simple two-phase microstructure of ZnO grain and a Pr oxide intergranular phase. In comparison with ZnO–Bi_2O_3-based varistors, which have spinel phase that play no significant electrical role, this two-phase microstructure increases the active grain boundary area through which electrical current flows [4, 5]. Since the discovery of ZnO-Pr_6O_{11} based varistors, a number of papers about ZnO-Pr_6O_{11} based varistors have been published, in which the doping effects of rare earth metal oxides such as Er_2O_3, Y_2O_3, La_2O_3 and Tb_4O_7 [6-8], or other metal oxides such as Fe_2O_3 [4], SnO_2 [5], Sb_2O_3 [9], and TiO_2 [10], or alkali ions [11, 12] on the microstructural and electrical properties of ZnO–Pr_6O_{11} based varistors have been well studied, but the breakdown voltages of most varistors reported were about 500 $V \cdot mm^{-1}$ or below. For super-high-voltage power transmission systems, however, it is known that higher breakdown voltage for varistors is also very important, because the increase of varistor voltage contributes to decrease the size of the varistor bulks, implying the economic use of materials and easy control of the scale of equipments. Therefore, it is not only useful but also necessary to explore ZnO varistors with high breakdown voltage.

For ZnO varistors, the breakdown voltages are directly proportional to the size of ZnO grains. The smaller the ZnO grains, the higher the varistor voltage. The growth of ZnO grains could be effectively controlled by

adjusting the ZrO_2 doping content in ZnO–Bi_2O_3 system, which enabled a wide-range adjustment of varistor voltage [1]. Furthermore, during modern ceramics processing, high energy attrition milling and ZrO_2 grinding media were often applied. As a result, Zr^{4+} contamination in ceramic samples is a common phenomenon. However, up to now no literature about the role of Zr^{4+} ion (ZrO_2) in ZnO–Pr_6O_{11}-based varistor has been reported. So, the aim of this work is to investigate the doping effect of ZrO_2 on the microstructural and the electrical properties of ZnO–Pr_6O_{11}-based varistor ceramics. It was found that while the nonlinear coefficient can be kept at quite high level, the breakdown voltage of ZnO-Pr_6O_{11}-based varistor ceramics could be greatly increased by doping with an appropriate amount of ZrO_2.

EXPERIMENTAL

Sample preparation

The samples were fabricated using a conventional ceramic processing method [4, 5] with a nominal composition of (98.0-x) mol. % ZnO + 0.5 mol.% Pr_6O_{11} + + 1.0 mol.% CoO + 0.5 mol.% Cr_2O_3 + x mol.% ZrO_2 (x = 0.0; 0.25; 0.5; 1.0; 2.0). All raw materials are commercial powders of analytical reagent grade. During processing, for the sample of each composition, the raw powders were first mixed and ball-milled in deionized water for at least 24 h so that the average grain size of ZnO was no more than 0.3 μm. After milling, the resultant slurries were dried in air at 120°C. After drying, the chunks of powder mixture were crashed into fine powders, and then sieved, resulting in ZnO composite powder with average granular size of no more than 10 μm. After that, discs of 6 mm in diameter and 1.5 mm in thickness were pressed from the prepared composite powders, yielding green bodies with density between 2.5 to 3.5 g·cm^{-3}. The samples were then sintered in a muffle oven at 1300°C for 2 h with heating rate of 2°C·min^{-1} and natural cooling. In order to measure the electrical properties, the sintered samples were coated on both sides with silver pastes and toasted at 500°C.

Materials characterization

The linear shrinkage in sample diameter was calculated as the percentage of the diameter difference between the green and sintered ones. The bulk density of the as-prepared samples was measured by Archimedes method according to international standard (ISO18754). The phase composition of the samples was identified by X-ray diffractometer (XRD, D/max2550HB+/PC, Cu Kα, and λ = 1.5418 Å) using a continuous scanning mode with speed of 8°·min^{-1}. To investigate the microstructure of the varistor ceramics, either of the sample surfaces was lapped and ground with SiC paper, and polished with 0.3 μm Al_2O_3 powder paste to a mirror-like finish, and then the samples were thermally etched at 1100°C for 30 min. The etched surface was examined with a scanning electron microscope (SEM, Model: SSX-550) equipped with an energy dispersive X-ray spectroscope (EDS). The average size of ZnO grains was determined from the SEM images using the linear intercept method.

The electric field vs current density (E–J) characteristics of the samples were recorded at room temperature with a high-voltage source measurement unit (Model: CJ1001). The varistor voltage was determined at 1 mA·cm^{-2} (V_{1mA}) and the leakage current (I_L) was determined at 0.75 V_{1mA}. Moreover, the nonlinear coefficient (α) was calculated using the following equation:

$$\alpha = \frac{\log(J_2/J_1)}{\log(E_2/E_1)} = \frac{1}{\log(E_2/E_1)} \quad (1)$$

where E_1 and E_2 are the electric fields corresponding to J_1 = 1 mA·cm^{-2} and J_2 = 10 mA·cm^{-2}, respectively.

The capacitance–voltage (C–V) characteristics of the varistor ceramics were measured at 1 kHz using Keithley 4200-SCS recorder. The donor density (N_d) of ZnO grains and the barrier height (φ_b) at the grain boundary were determined by the following equation [5]:

$$\left(\frac{1}{C} - \frac{1}{2C_0}\right)^2 = \frac{2t}{A^2\, d\, e^{\varepsilon}\, N_d} V + \frac{2t^2}{A^2\, d^2\, e^{\varepsilon}\, N_d} \Phi_b \quad (2)$$

where C_0 and C are the corresponding capacitances of the samples under different applied voltages, in which C_0 is the value of C when V = 0, and V is the applied voltage; t is the thickness of the specimens, A is the electrode area of specimen, and d is the average grain size; and ε is the permittivity of ZnO, and e is electron charge.

RESULTS AND DISCUSSION

Sinterability

Figure 1 shows the average linear shrinkages in diameter and bulk densities of the as-prepared varistor ceramics doped with different amounts of ZrO_2. The diameter shrinkage decreased with increasing ZrO_2 doping contents in the varistor ceramics, which implies that the ZrO_2 doping works against the sintering (densification) of the samples. However, the sample density first increased as the doping content of ZrO_2 increased up to 0.5 mol. %, and then decreased with further increasing doping of ZrO_2. The increase of the density might be mainly attributed to the replacement of the lighter Zn atoms by heavier Zr ones; but the decrease of the average size of ZnO grains (see the discussion in next section) might be also a positive factor to certain extent for the densification of the samples [13, 14]. The decrease of the sample density is correlated with the decrease of the sample shrinkage; and the formation of more pores in the microstructures (see next section), due to the worse sinterabilities of the samples doped with more ZrO_2.

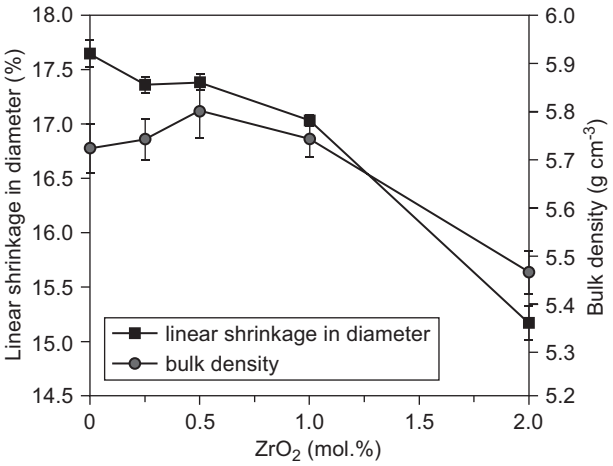

Figure 1. Average linear shrinkages in diameter and bulk densities of the as-prepared ZnO–Pr_6O_{11}–CoO–Cr_2O_3-based varistor ceramics doped with different amounts of ZrO_2.

Composition and microstructure

Typical XRD patterns with normalized peak intensity of the as-prepared varistor ceramics doped with different amounts of ZrO_2 are presented in Figure 2. From this figure it can be seen that, without ZrO_2 doping only the phases of ZnO and praseodymium oxides (both cubic Pr_2O_3 and hexagonal Pr_6O_{11}) were identified. The cubic Pr_2O_3 phase was formed due to the decomposition of the applied hexagonal Pr_6O_{11} at high temperature during sintering. However, after certain amount of ZrO_2 was added, a new phase $Pr_2Zr_2O_7$ was detected, which is obviously a result of the sintering reaction between ZrO_2 and praseodymium oxides. With the increase of ZrO_2 doping contents in the ceramics, it could be observed that the relative intensity of praseodymium oxide phases decreased and that of $Pr_2Zr_2O_7$ became much stronger.

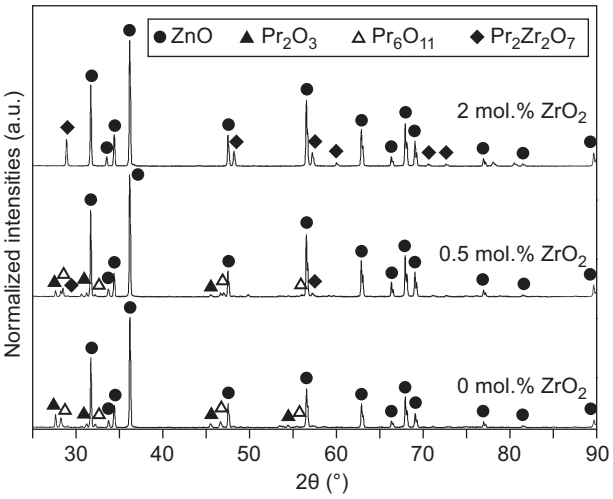

Figure 2. Typical XRD patterns of the as-prepared ZnO–Pr_6O_{11}–CoO–Cr_2O_3-based varistor ceramics doped with different amounts of ZrO_2.

In particular, when the ZrO_2 doping content was high enough (1.0 mol. % in this work), the praseodymium oxide phases were almost absent in the XRD patterns. The reason for this phenomenon might be that the

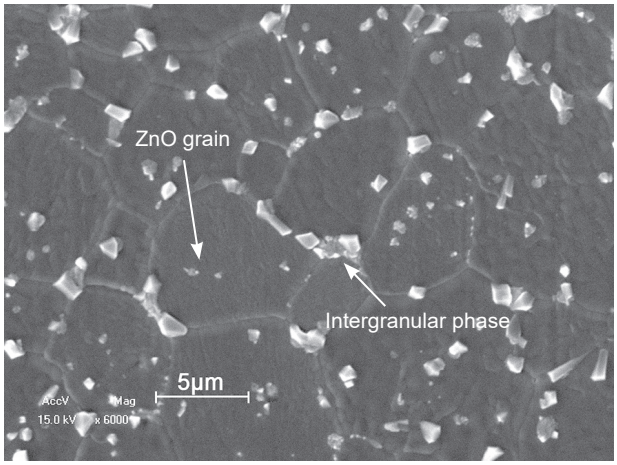

a) 0 mol. % ZrO_2

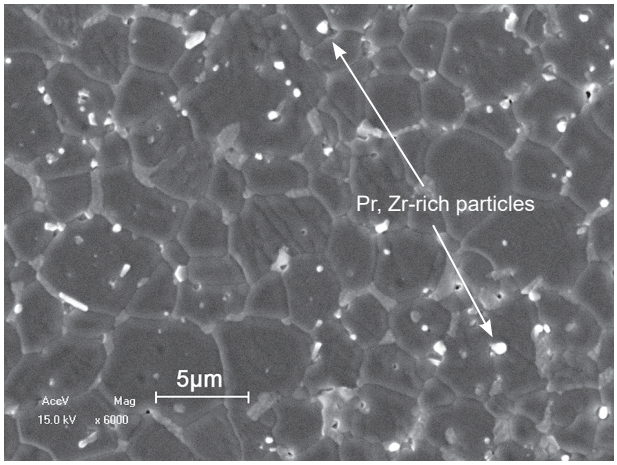

b) 0.5 mol. % ZrO_2

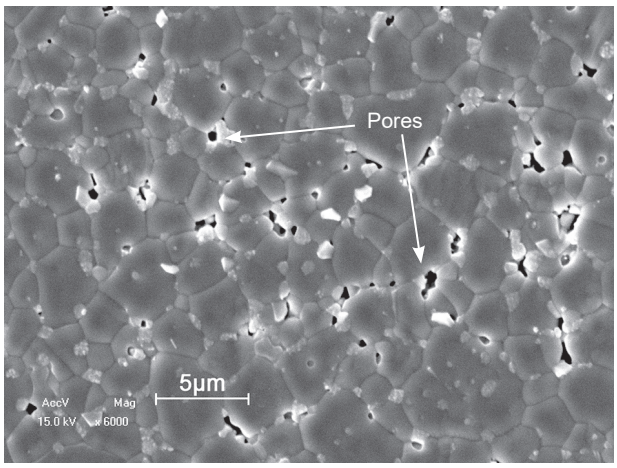

c) 2.0 mol. % ZrO_2

Figure 3. Typical SEM images of the as-prepared ZnO–Pr_6O_{11}–CoO–Cr_2O_3-based varistor ceramics doped with different amounts of ZrO_2: a) 0 mol. % ZrO_2; b) 0.5 mol. % ZrO_2; c) 2.0 mol. % ZrO_2.

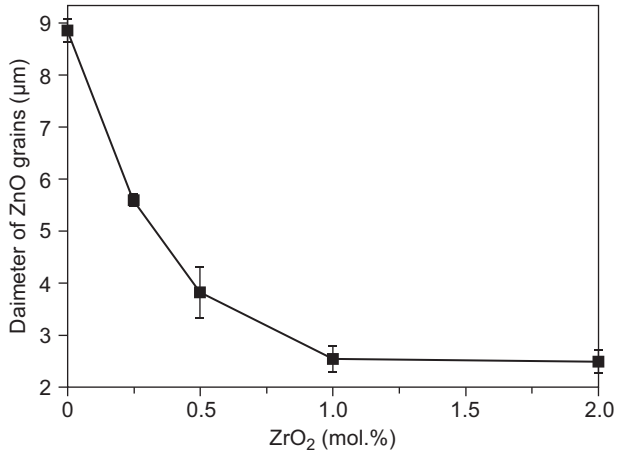

Figure 4. Average ZnO grain sizes calculated from the previous SEM images in Figure 3.

majority of praseodymium oxides was engaged into the sintering reaction with the doped ZrO_2, resulting in the above-mentioned $Pr_2Zr_2O_7$ phase, which was stable at the high temperature of sintering. In addition, although other dopants of CoO and Cr_2O_3 were applied, no peaks of them were identified, possibly because their doping amounts were too small, or they were entering into the lattices of ZnO grains after sintering (thus no independent peaks appeared).

Figure 3 displays typical SEM images of the prepared varistor ceramics doped with different amounts of ZrO_2. It is well known that the microstructure of ZnO–Pr_6O_{11}-based varistor ceramics consists of only two phases, ZnO and intergranular phase. After comparing with the EDS results, one can find from this figure that the doping of ZrO_2 would not change the typical microstructure of ZnO-Pr_6O_{11}-based varistor ceramics. Combined with the results determined by XRD analysis as shown in Figure 2, it can be concluded that the bulk phase in the microstructure of the as-prepared varistor ceramics is ZnO, and the white intergranular phases are praseodymium oxides and $Pr_2Zr_2O_7$. Moreover, from these SEM images, it can be clearly seen that with increasing ZrO_2 contents in the ceramics, the average size of ZnO grains decreases, which is also evident from the calculated average size of ZnO grains as illustrated in Figure 4. The reason for the decrease in ZnO grain size of the as-prepared varistor ceramics may be attributed to the formation of secondary phase $Pr_2Zr_2O_7$ during sintering, which would pin at the boundary of ZnO grains, thus hindering the growth of ZnO grains. However, due to the worse sinterability of the samples, more and more pores were clearly observed when too much more ZrO_2 was doped into the ceramics, which is harmful to the densification and electrical properties of the samples.

C–V characteristics

The *C–V* characteristics of the as-prepared ZnO-Pr_6O_{11}–CoO–Cr_2O_3-based varistors doped with different amounts of ZrO_2 are shown in Figure 5a. The related C–V characteristic parameters of the varistor samples calculated from it including donor density and barrier height were illustrated in Figure 5b. Compared with the sample without ZrO_2, the donor density of all the samples with ZrO_2 doping, regardless of the ZrO_2 doping contents, all decreased. Thus it is believed that the doped ZrO_2 acted as acceptor in ZnO-Pr_6O_{11} based varistor. Moreover, it was reported that the donor density could directly influence the barrier height of varistors [5]. So, the doping of ZrO_2 could directly change the barrier height of ZnO–Pr_6O_{11}–CoO–Cr_2O_3-based varistors. From Figure 5b, it can be seen that the barrier height of the as-prepared ceramic varistors initially increased

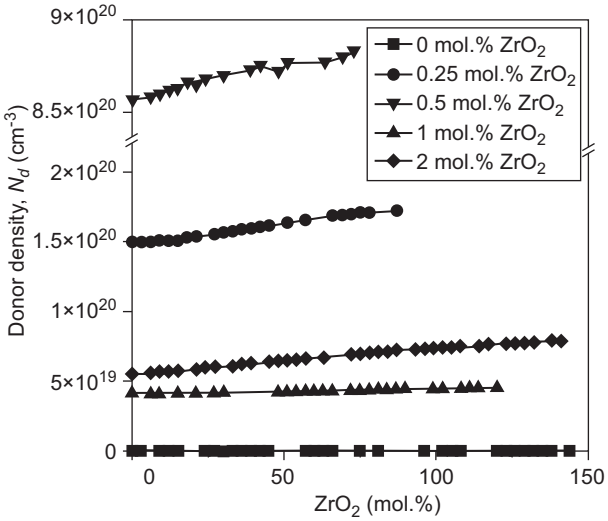

a)

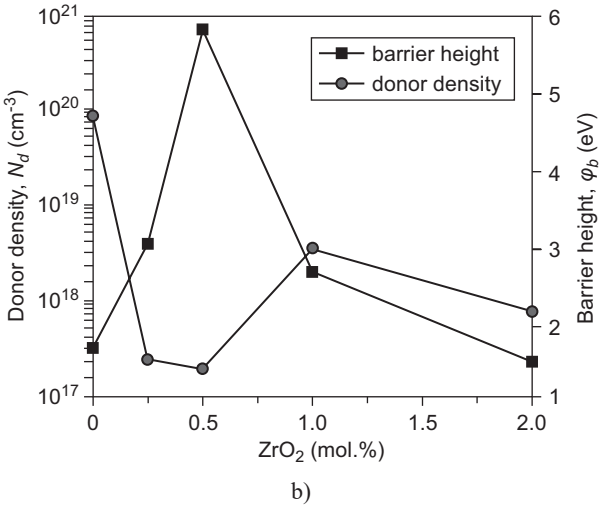

b)

Figure 5. C–V characteristics of the as-prepared ZnO–Pr_6O_{11}–CoO–Cr_2O_3-based ceramic varistors doped with different amounts of ZrO_2 (a) and the donor density and barrier height calculated from C-V characteristic curves (b).

with small doping content of ZrO_2 up to 0.5 mol. %, and then decreased with further increasing ZrO_2 doping. In this study the sample doped with 0.5 mol. % ZrO_2 presented the largest barrier height. Because the increase of barrier height is in favor of the raise of varistors' nonlinear coefficient, so it is believed that the samples doped with 0.5 mol. % ZrO_2 would possess a relatively high nonlinear coefficient, which is consistent with the results presented in next section.

E-J characteristics

The *E-J* characteristics of the as-prepared ZnO–Pr_6O_{11}–CoO–Cr_2O_3-based ceramic varistors doped with different amounts of ZrO_2 are presented in Figure 6a. Their corresponding electrical parameters calculated from the *E-J* curves are illustrated in Figure 6b.

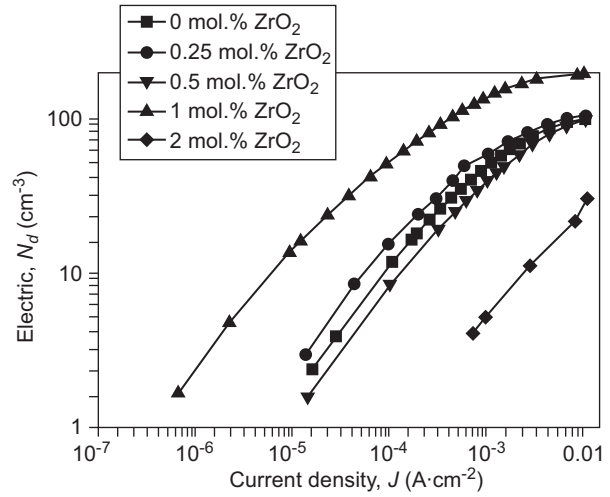

a)

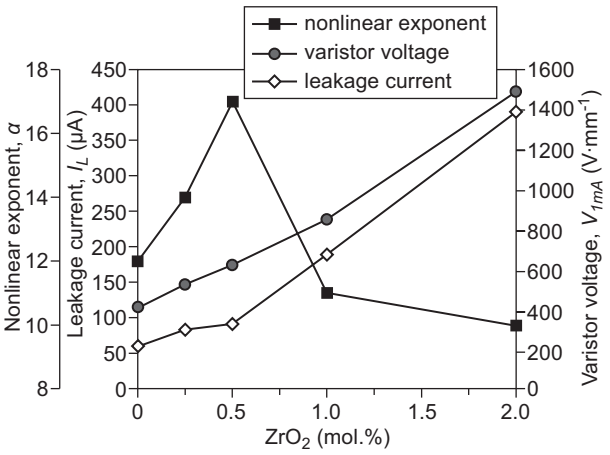

b)

Figure 6. E-J characteristics of the as-prepared ZnO–Pr_6O_{11}–CoO–Cr_2O_3-based ceramic varistors doped with different amounts of ZrO_2 (a) and the varistor parameters calculated from E-J characteristic curves (b).

From Figure 6b, it can be seen that the varistor voltage of the samples increased from 411 to 1490 V·mm^{-1} when the doping content of ZrO_2 in them increased from 0.0 to 2.0 mol. %. The increase of varistor voltage can be attributed to the increasing number of grain boundaries owing to the decrease of average ZnO grain size [1,4].

When the doping amount of ZrO_2 was no more than 0.5 mol. %, the nonlinear exponent increased with the increase of ZrO_2 content in the ceramic varistors; but the nonlinear exponent decreased when more ZrO_2 was doped. The increase of the nonlinear exponents might be attributed to the increase of barrier height of the samples, which is consistent with the C–V analysis in the last section that the barrier height increased with the increase of ZrO_2 doping contents up to 0.5 mol. %. The decrease of the nonlinear exponents might be correlated to the excessive decrease of the content of praseodymium oxides in the ceramic varistors due to the reaction between praseodymium oxides and ZrO_2 into $Pr_2Zr_2O_7$, consuming out the VFO. This is consistent with results reported by literature that in sintering, praseodymium oxides provided for the formation of insulating boundary layers which controlled the operation of varistors [4, 5]. So, it is believed that the consumption of a large number of praseodymium oxides by such sintering reaction will be adverse to the formation of insulating boundary layers. Furthermore, there would be more pyrochlore phase $Pr_2Zr_2O_7$ formed when more ZrO_2 was doped. The $Pr_2Zr_2O_7$ phase, which would segregate at grain boundary, might also destroy the insulating boundary layers. Therefore, the consumption of a large number of praseodymium oxides and the mass formation of $Pr_2Zr_2O_7$ might be the primary cause for the decrease of the nonlinear exponents when the ZrO_2 doping amounts were more than 0.5 mol. %.

The leakage currents increased with the increase of ZrO_2 doping contents, due to the deteriorating sinterability of the samples after ZrO_2 doping, which resulted in continuously increased amount of pores in the ceramics after more and more ZrO_2 was doped. This is the decisive factor for the increase in the leakage current of the prepared varistor [1, 15].

The optimum nonlinear electrical properties were obtained in samples doped with about 0.5 mol. % ZrO_2, whose varistor voltage and nonlinear coefficient were 623 V·mm^{-1} and 17, respectively. Samples doped with 2.0 mol. % ZrO_2 reached the highest varistor voltage in this study, which was about 1490 V·mm^{-1}, and its nonlinear exponent was about 10. Such kind of ceramic varistors of high breakdown voltage would be very promising in super-high-voltage power transmission systems.

CONCLUSIONS

The microstructure of ZrO_2-doped ZnO–Pr_6O_{11}-based varistor ceramics was composed of two phases, ZnO grain and intergranular phase. The doping of ZrO_2

can inhibit the growth of ZnO grains, due to the formation of $Pr_2Zr_2O_7$, resulting in greatly increased varistor voltages. Minor doping of ZrO_2 up to 0.5 mol. % can improve the nonlinear exponents of the ceramic varistors.

Acknowledgments

The authors would like to thank the financial support for this work from the National Natural Science Foundation of China (Grant Nos. 61274015, 11274052 and51172030), and Excellent Adviser Foundation in China University of Geosciences from the Fundamental Research Funds for the Central Universities.

REFERENCES

1. Jiang F., Peng Z. J., Zang Y. X., Fu X. L.: J. Adv. Ceram. *2*, 201 (2013).
2. Ke L., Yuan Y. H., Zhao H., Ma X.M.: Ceramics-Silikaty *57*, 53 (2013).
3. Wang M. H., Zhao Z. Y., T. T. Liu: J. Alloys Compd. *621*, 220 (2015).
4. Peng Z. J., Fu X. L., Zang Y. X., Fu Z. Q., Wang C. B., Qi L. H., Miao H. Z.: J. Alloys Compd. *508*, 494 (2010).
5. Feng H., Peng Z. J., Fu X. L., Fu Z. Q., Wang C. B., Qi L. Q., Miao H. Z.: J. Alloys Compd. *509*, 7175 (2011).
6. Nahm C. W.: Ceram. Int. *40*, 12561 (2014).
7. Nahm C. W.: J. Rare Earths *30*, 1028 (2012).
8. Nahm C. W.: J. Rare Earths *31*, 276 (2013).
9. Peng S. J., Wang Y., Wang H. Q., Dong X., Dong L., Gan Y. J. : J. Am. Ceram. Soc. *95*, 2914 (2012).
10. Feng H., Peng Z. J., Fu X. L., Fu Z. Q., Wang C. B., Qi L. H., Miao H. Z.: J. Alloys Compd. *497*, 304 (2010).
11. Peng Z. J., Jiang F., Feng H., Fu X. L.: Key Eng. Mater. *544*, 213 (2013).
12. Mei L. T., Hsiang H. I., Hsi C. S., Yen F. S.: J. Alloys Compd. *558*, 84 (2013).
13. Peng Z. J., Wang C. B., Gauckler L. J., Miao H. Z.: Key Eng. Mater. *368-372*, 479 (2008).
14. Fu X. L., Tang W. H., Peng Z. J.: Acta Phys. Sin. *57*, 5844 (2008).
15. Gupta T. K.: J. Am. Ceram. Soc. *73*, 1817 (1990).